DOI 10.5012/bkcs.2010.31.11.3259

Amperometric Immunosensor for Myeloperoxidase in Human Serum Based on a Multi-wall Carbon Nanotubes-Ionic Liquid-Cerium Dioxide Film-modified Electrode

Lingsong Lu, Bei Liu, Chenggui Liu, and Guoming Xie*

*Key Laboratory of Medical Diagnostics of Ministry of Education, Department of Laboratory Medicine, Chongqing Medical University, Chongqing 400016, P. R. China. *E-mail: guomingxie@cqmu.edu.cn*
Received July 6, 2010, Accepted September 14, 2010

A label-free amperometric immunosensor has been proposed for the detection of myeloperoxidase (MPO) in human serum. To fabricate such an immunosensor, a composite film consisting of N,N-dimethylformamide (DMF), multi-wall carbon nanotubes (MWCNTs) and 1-ethyl-3-methyl imidazolium tetrafluoroborate ($EMIMBF_4$) suspension was initially formed on a glassy carbon electrode (GCE). Then cerium dioxide (CeO_2) dispersed by chitosan was coated on the GCE. After that, MPO antibodies (anti-MPO) were attached onto the nanoCeO_2 surface. With a noncompetitive immunoassay format, the antibody-antigen complex formed between the immobilized anti-MPO and MPO in sample solution. The immunosensor was characterized by cyclic voltammetry, transmission electron microscopy (TEM) and scanning electron microscopy (SEM). The factors influencing the performance of the immunosensor were studied in detail. Under optimal conditions, the current change before and after the immunoreaction was proportional to MPO concentration in the range of 5 to 300 ng mL^{-1} with a detection limit of 0.2 ng mL^{-1}.

Key Words: Myeloperoxidase, Ionic liquid, Carbon nanotubes, Cerium dioxide, Immunosensor

Introduction

Myeloperoxidase (MPO) is an abundant mammalian phagocyte hemoprotein that is in culprit lesions of individuals with sudden cardiac death, such as those found in human atheroma thought to be a potential participant in multiple phases of the atherosclerotic process.[1,2] Nowadays it has been discovered that there was a close relationship between MPO and the unstability of atherosclerotic plaque.[3,4] The rupture of atherosclerotic plaque is the common pathology inducement to the majority of acute coronary syndrome (ACS).[5] In patients with ACS, MPO serum levels powerfully predict an increased risk for subsequent cardiovascular events and extend the prognostic information gained from traditional biochemical markers.[6] It is usually to detect the concentration of cTnI, Myo and CK-MB in human serum to distinguish vulnerable atheroma clinically, but they all obviously changed after the occurrence of myocardial infarction (MI). However, a single initial measurement of plasma myeloperoxidase independently predicts the early risk of myocardial infarction (MI), as well as the risk of major adverse cardiac events in the ensuing 30-day and 6-month periods.[7] Therefore, it is very important to detect MPO promptly to avoid the occurrence of ACS.

Some analytical methods including enzyme-linked immunosorbent assay (ELISA) and radio- immunoassay (RIA) have been employed to detect MPO. However, these methods have some drawbacks such as complicated and time-consuming procedures, radiation hazards and requirement for qualified workers and sophisticated instruments. When it comes to electrochemical immunosensors, they have been considered suitable for MPO detection due to advantages such as simple pretreatment procedure, fast analytical time, highly sensitive current measurement, lower price and portability.[8-10]

In the electrochemical immunoassays, the key point lies in the fabrication of the immunosensors. Some promising materials have been applied to construct the immunosensors. Nanomaterials such as gold nanoparticles,[11,12] platinum nanoparticles,[13,14] zinc oxide[15,16] and titanium oxide[17,18] often used as a binder to immobilize biomolecules like enzymes or antibodies due to their unique properties such as good biocompatibility, high surface-to-volume ratio, which have attracted much interest in the construction of immunosensors. Nowadays, cerium dioxide (CeO_2) has been reported as a potential candidate material for the immobilization of the desired biomolecules due to its unique properties of large surface area and strong adsorption ability.[19-22] The high isoelectric point (IEP~9.2) of CeO_2 can be helpful to immobilize desired antibodies of low IEP *via* electrostatic interactions. Furthermore, the low price of cerium dioxide is more competitive than gold nanoparticles.[23] Feng *et al.* have prepared a nanoporous CeO_2/chitosan composite matrix for the immobilization of single-stranded DNA probes for the detection of cancer genes.[24] Anees A *et al.* have fabricated an amperometric biosensor employing sol-gel derived nano-structured cerium oxide (NS-CeO_2) film as matrix to immobilize the Cholesterol oxidase.[25]

Recently, room temperature ionic liquids (RTILs) have been reported to have promising applications in the fabrication of the biosensors,[26] which have drawn significant interest because of its unique properties such as negligible vapor pressure, wide potential windows, high thermal stability and viscosity, good conductivity and solubility.[27] Zhang *et al*. used 1-butyl-3-methylimidazolium hexafluorophosphate ($BMIMPF_6$) supported CeO_2 nanoshuttles-carbon nanotubes composite as a platform for impedance DNA hybridization sensing in hope of enhancing the sensitivity of the biosensor.[28] Despite some advantages of $BMIMPF_6$, it can't be well dissolved in DMF. The

hydrophobicity confined the joint use of $BMIMPF_6$ and some water-solubility materials. In the present paper, we substituted $BMIMPF_6$ to $EMIMBF_4$. $EMIMBF_4$ is a kind of hydrophil RTILs, not only possesses all the merits of RTILs, but also can be well dissolved in DMF. Furthermore, spherical CeO_2 has larger surface-to-volume ratio and stronger adsorption ability than CeO_2 nanoshuttles, so more anti-MPO can be loaded on per unit mass of particles. On the other hand, MWCNTs have received wide attention as an electrode modification material, which was widely used in electrochemistry and electroanalytical chemistry. The considerable interest is due to the remarkable properties of MWCNTs, including high electrical conductivity, chemical stability and electrocatalytic property.[29,30] To sum up, considering the advantages of $EMIMBF_4$ and MWCNTs above, we obtained a suspension by dispersing MWCNTs in DMF-$EMIMBF_4$, which was used as matrix in this study.

In addition, chitosan is a kind of attractive natural polymer, which has been applied to immobilize biomolecules due to its excellent characteristic properties such as membrane-forming ability, remarkable adhesion and good biocompatibility. It is also commonly used to disperse nano-materials for constructing biosensors.[31,32] In this work, chitosan was selected to disperse nanoCeO_2 and provide a good biocompatible microenvironment for anti-MPO.

In this paper, we proposed an amperometric immunosensor by immobilizing anti-MPO onto the composite film composed of DMF-MWCNTs-$EMIMBF_4$, chitosan-nanoCeO_2, successively coated on a glassy carbon electrode (GCE), which was used to detect MPO. The experimental results indicated that $EMIMBF_4$ and MWCNTs could efficiently improve the electron transfer between the composite film and the electrode. Chitosan-nanoCeO_2 film was used as a binder to adsorb anti-MPO, providing a good microenvironment for the immobilization of more anti-MPO. The preparation and characterization of the immunosensor were investigated. Moreover, the factors influencing the performance of the obtained immunosensor were also discussed in detail.

Experimental

Chemicals. Room temperature ionic liquid, 1-ethyl-3-methylimidazolium tetrafluoroborate (≧ 99%, $EMIMBF_4$) was purchased from Lanzhou Institute of Chemical Physics, Chinese Academy of Sciences. (Lanzhou, China). N,N-dimethylformamide (DMF) was purchased from Shanghai Sinopharm Group Chemical Reagent Co., Ltd. (Shanghai, China). Functionalized MWCNTs was obtained from Shenzhen Nanotech Port Co., Ltd. (Shenzhen, China). NanoCeO_2 (spherical, particle diameter: 20 nm) was obtained from Beijing Nachen S&T Co. (Beijing, China). MPO, anti-MPO, chitosan (purity≧90%) and Bovine serum albumin (BSA, 96 - 99%) were obtained from Sigma (USA). Serum specimens were gifted by the First Affiliated Hospital, Chongqing Medical University. Double distilled water was used for all experiments. All reagents were of analytical grade unless otherwise stated.

Apparatus. A μAUTOLAB III Electrochemistry Workstation (Eco Chemie, Netherlands) was used for cyclic voltammetric measurements. A three electrode system was consisted of a modified glassy carbon electrode; (GCE, Φ = 4 mm) as the working electrode, platinum (Pt) wire as the auxiliary electrode and Ag/AgCl as the reference electrode. The transmission electron microscopy (TEM) was carried out on a Hitachi-7500 Transmission Electron Microscope (Hitachi, Japan). Scanning electron microscopy (SEM) was carried out using a Hitachi S-4800 Scanning Electron Microscope (Hitachi, Japan).

Preparation of chitosan-CeO_2, DMF-MWCNTs-$EMIMBF_4$ suspension. Chitosan solution (0.5%, w/w) was prepared by dissolving chitosan powder in acetic acid solution (1.0%, v/v) with stirring for 1 h at room temperature until completely dispersed. After that, appropriate amount of nano-sized CeO_2 was dispersed in chitosan solution with a mass ratio of 50:1 (chitosan: CeO_2), sonicated for about 2 h. Then the chitosan-CeO_2 suspension was obtained.

5.0 mg MWCNTs were dispersed in 5.0 mL DMF and sonicated for 2 h. After that, 40.0 μL $EMIMBF_4$ (2.0%, v/v) was dispersed in the DMF-MWCNTs with the aid of ultrasonication for 30 min. Then the DMF-MWCNTs-$EMIMBF_4$ homogeneous suspension was obtained.

Fabrication of the immunosensor. The glassy carbon electrode was successively polished to a mirror-like surface with 0.3 μm and 0.05 μm alumina. Following that, the electrode was rinsed by double distilled water. Then, the electrode was sonicated in double distilled water, ethanol and double distilled water for 5 min, respectively. Then 6.0 μL of the DMF-MWCNTs-$EMIMBF_4$ suspension was dropped onto the cleaned GCE to form a uniform membrane. After the electrode was dried at room temperature, 5.0 μL chitosan-CeO_2 suspension was coated on the electrode. Then, the chitosan-CeO_2/DMF-MWCNTs-$EMIMBF_4$ homogeneous composite film was obtained and let it dry at room temperature. After rinsed by double distilled water, the modified electrode was dipped into the anti-MPO solution at 4 °C overnight. Finally, the BSA (1%, w/w) solution was used to block the remaining active groups of the nanoCeO_2 for 2 h at room temperature. The finished immunosensor was stored at 4 °C when not in use. Fabrication procedure of the immunosensor was illustrated in Scheme 1.

Electrochemical measurement. The electrochemical characterizations and measurements on the modified electrode were carried out using cyclic voltammetry from −0.2 to 0.8 V (*versus* Ag/AgCl) in 5.0 mmol L^{-1} $K_3[Fe(CN)_6]/K_4[Fe(CN)_6]$ with 0.1 mol L^{-1} KCl solution (pH 7.0) at 50 mV s^{-1}. The fabricated immunosensors were incubated in various concentrations of MPO solution at 37 °C for 10 min to obtain a antigen-antibody complex layer. The amperometric detection of the MPO level was based on the change of the peak current response before and after the antigen-antibody reaction. All the measurements

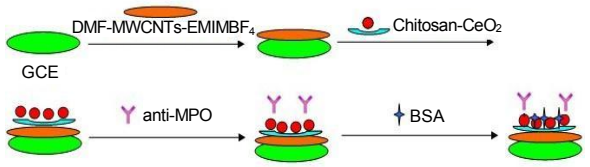

Scheme 1. Fabrication process of the developed immunosensor

were performed under the optimum conditions.

Results and Discussions

TEM images of carbon nanotubes in different solvents and SEM images of different modified electrodes. Fig. 1(a) shows that MWCNTs were dispersed in DMF but the MWCNTs were a little entangled. As shown in Fig.1(b), when $EMIMBF_4$ was introduced in DMF-MWCNTs suspension, MWCNTs were uniformly distributed over DMF-$EMIMBF_4$. The entangled nanotube bundles were found to untangle within the suspension to form much finer bundles. This is because the interaction between π electrons of the MWCNTs surface and cations of the ionic liquid could orient imidazolium ions on MWCNTs surface and trigger more likely a lot of weak physical network among the MWCNTs bundles.[33] The morphological features of the different modified electrodes were studied by means of scanning electron microscopy (SEM). The morphology of the chitosan-CeO_2/DMF-MWCNTs-$EMIMBF_4$/GCE could be observed that GCE surface was mostly covered with homogenous MWCNTs, $EMIMBF_4$ and many spherical CeO_2 particles, confirming the formation of chitosan-CeO_2/DMF-MWCNTs-$EMIMBF_4$ composite membrane in Fig. 1(c). When anti-MPO was adsorbed onto the chitosan-CeO_2/DMF-MWCNTs-$EMIMBF_4$ film in Fig. 1(d), the surface morphology became smoother, which might be ascribed to anti-MPO filling the interstitial places on the above interface. The result indicated that an anti-MPO layer was well-linked to the surface of chitosan-CeO_2/DMF-MWCNTs-$EMIMBF_4$ film.

Electrochemical behavior of the immunosensor. To investigate the effect of different materials on the electrochemical behavior of the immunosensor, cyclic voltammograms of differently modified electrodes were recorded from −0.2 to 0.8 V in 5.0 mmol L^{-1} $K_3[Fe(CN)_6]/K_4[Fe(CN)_6]$ with 0.1 mol L^{-1} KCl solution (pH 7.0) at 50 mV s^{-1}. A pair of well-defined peaks is shown in Fig. 2(a), which reflects the reversible redox reaction of ferricyanide ions on the bare glassy carbon electrode. When the DMF-MWCNTs suspension was coated on the electrode surface, a stable and reversible redox peak is shown in Fig. 2(b), demonstrating the efficient electroactive performance and excellent conductivity of MWCNTs. Then the redox peak obviously increased (Fig. 2(c)) after MWCNTs dispersed in DMF-$EMIMBF_4$ was coated onto the electrode surface. Apparently, the oxidation peak became well-defined and sharp, with a negative potential shift of 20 mV. The lower overpotential and the increase in current response are clear evidence of the fact that $EMIMBF_4$ greatly facilitates electron transfer. A further increase of the peak current (Fig. 2(d)) was obtained after Chitosan-CeO_2 suspension was coated onto the composite membrane, resulting from the formation of the conductive Chitosan-CeO_2 film, which indicated that the Chitosan-CeO_2 film enhanced the electrochemical response of the $[Fe(CN)_6]^{4-/3-}$. This was attributed to the excellent electronic conductivity of cerium oxide. After the anti-MPO was successfully loaded onto the chitosan-CeO_2/DMF-MWCNTs-$EMIMBF_4$ composite film modified electrode, redox peak current decreased obviously (Fig. 2(e)), which suggested the protein anti-MPO severely reduced effective area and active sites for electron transfer. After BSA was used to block nonspecific sites, the transmission of ferricyanide to the electrode surface was hindered and peak current further decreased (Fig. 2(f)).

Effect of the pH, the incubation temperature and the incubation time. The experiment conditions that influenced the performance of the immunosensor including the pH of the supporting electrolyte, the incubation temperature and the incubation time have been discussed. The acidity of the supporting electrolyte greatly affected the antibody activity, which was investigated in Fig. 3(a). The current change increased with the increment of pH from 3.5 to 7.0 and then decreased. So we set the optimum pH at 7.0. The influences of the antigen-antibody

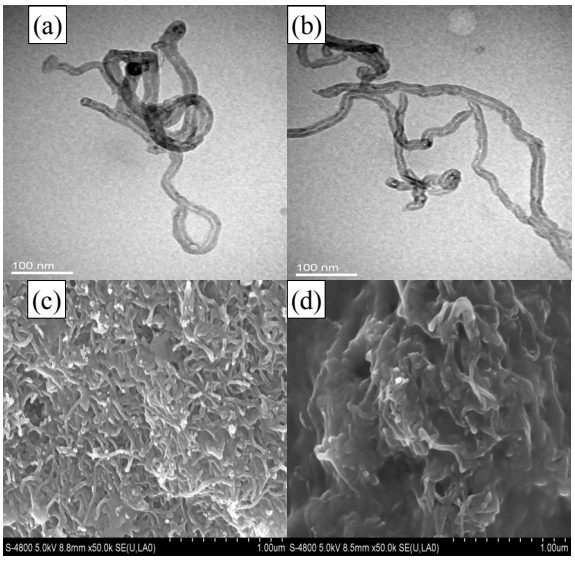

Figure 1. (a) TEM image of MWCNTs in DMF. (b) TEM image of MWCNTs in DMF-$EMIMBF_4$ composite suspension. (c) SEM image of chitosan-CeO_2/DMF-MWCNTs-$EMIMBF_4$/GCE. (d) SEM image of anti-MPO/chitosan-CeO_2/DMF-MWCNTs-$EMIMBF_4$/GCE.

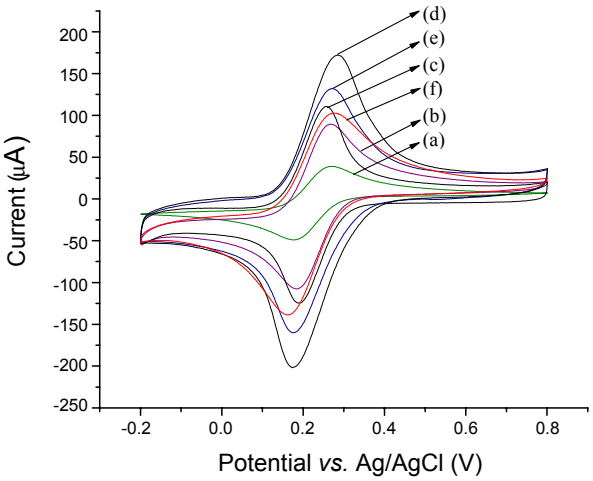

Figure 2. Cyclic voltammograms of (a) GCE, (b) DMF-MWCNTs/GCE, (c) DMF-$EMIMBF_4$- MWCNTs/GCE, (d) chitosan-CeO_2/DMF-$EMIMBF_4$-MWCNTs/GCE, (e) anti-MPO/chitosan-CeO_2/DMF-$EMIMBF_4$-MWCNTs/GCE, (f) BSA-anti-MPO/chitosan-CeO_2/DMF-$EMIMBF_4$-MWCNTs/GCE in 5.0 mmol L^{-1} $K_3[Fe(CN)_6]/K_4[Fe(CN)_6]$ with 0.1 mol L^{-1} KCl solution (pH 7.0). Scan rate: 50 mV s^{-1}.

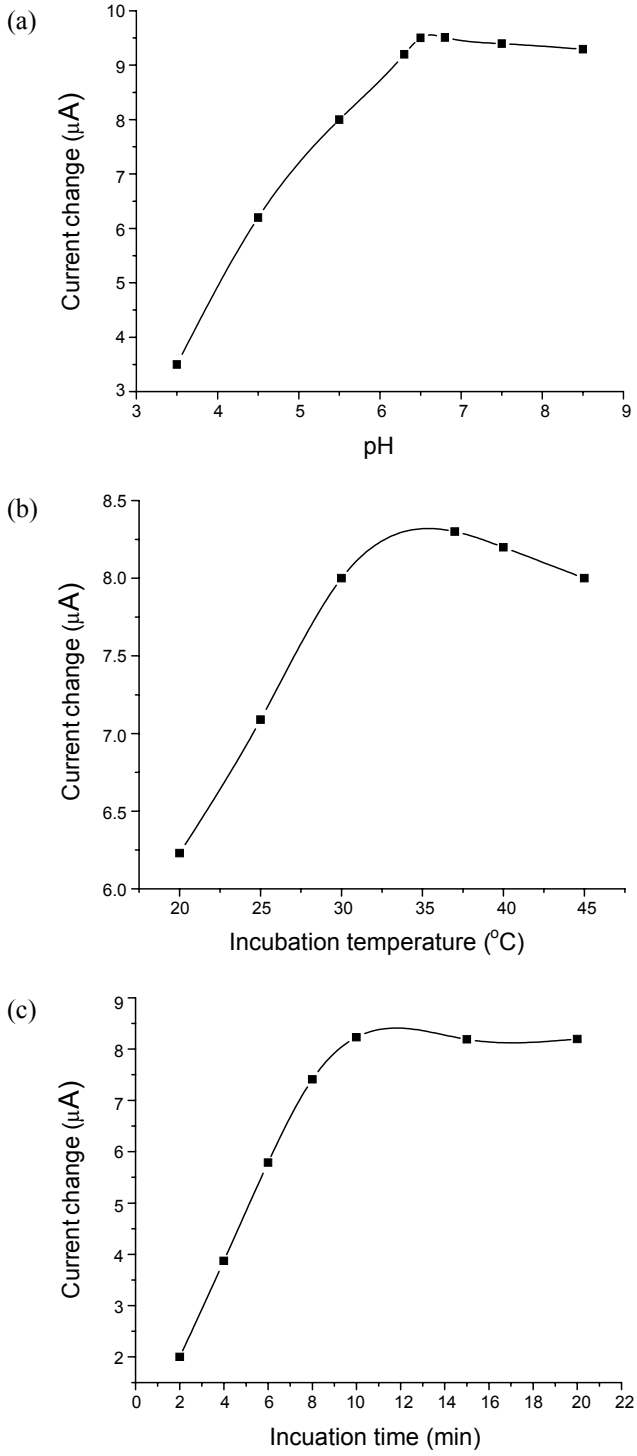

Figure 3. (a) Influence of the pH of supporting electrolyte on the immunosensor incubated with 100 ng mL^{-1} MPO in 5.0 mmol L^{-1} $K_3[Fe(CN)_6]/K_4[Fe(CN)_6]$ with 0.1 mol L^{-1} KCl solution at 50 mV s^{-1}. (b) Influence of incubation temperature on the immunosensor incubated with 100 ng mL^{-1} MPO in 5.0 mmol L^{-1} $K_3[Fe(CN)_6]/K_4[Fe(CN)_6]$ with 0.1 mol L^{-1} KCl solution (pH 7.0) at 50 mV s^{-1}. (c) Influence of incubation time on the immunosensor incubated with 100 ng mL^{-1} MPO in 5.0 mmol L^{-1} $K_3[Fe(CN)_6]/K_4[Fe(CN)_6]$ with 0.1 mol L^{-1} KCl solution (pH 7.0) at 50 mV s^{-1}.

incubation temperature on the amperometric responses were also studied. When the temperature achieved to 37 °C, we got

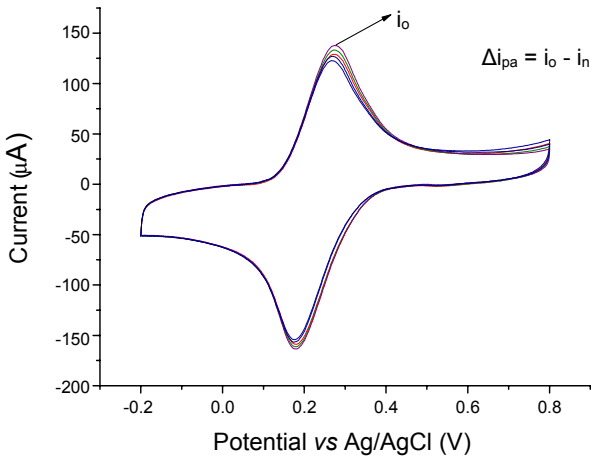

Figure 4. Cyclic voltammograms of the fabricated immunosensor in 5.0 mmol L^{-1} $K_3[Fe(CN)_6]/K_4[Fe(CN)_6]$ with 0.1 mol L^{-1} KCl solution (pH 7.0) at 50 mV s^{-1} : (i_0) without MPO, (i_n) with MPO at different concentration levels (from outter to inner): n = 20, 50, 80, 100 ng mL^{-1}.

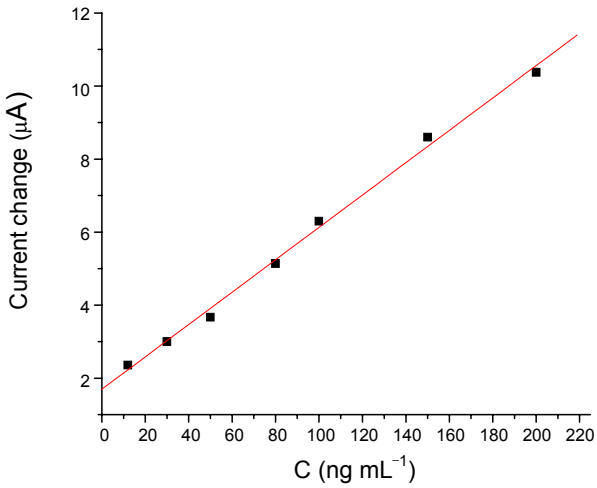

Figure 5. Calibration curve of the as-prepared immunosensor toward standard MPO samples.

the most obvious current change in Fig. 3(b). So the optimal temperature was 37 °C. Fig. 3(c) shows the influence of incubation time on the immunoassay. The modified immunosensors were immersed in 100 ng mL^{-1} MPO solution for 2, 4, 6, 8, 10, 15 and 20 min, respectively. The current change increased with the increment of incubation time from 2 to 10 min. The optimal current response was achieved when the incubation time was 10 min. Thus, 10 min was adopted as the optimal incubation time for subsequent study.

Response mechanism and calibration curve of the developed immunosensor. When the immunosensor was incubated in the MPO solution for 10 min, a dramatically decrease in current was observed (Fig. 4). This was attributed to the formation of anti-MPO/MPO immunocomplex, which acted as the inert electron and mass transfer blocking layer and hindered the diffusion of ferricyanide toward the electrode surface. The detection principle was based on the change of oxidation peak current response (Δi_{pa}) before and after the antibody-antigen

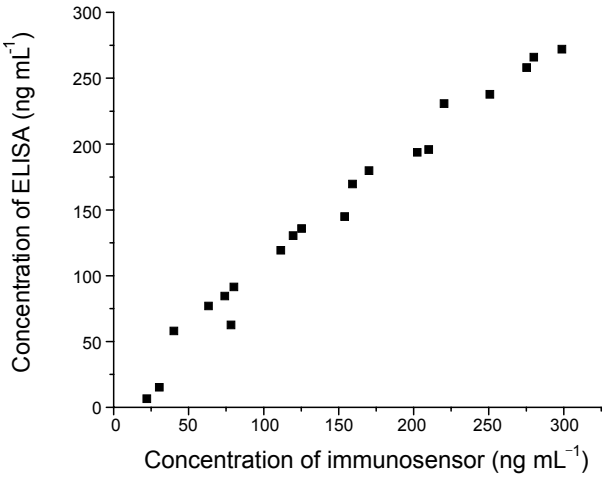

Figure 6. Scatterplot of correlation analysis about the developed immunosensor and standard ELISA method.

Table 1. Specificity of the immunosensor

samples	current (μA)	$(i_b-i_a)/i_a$ (100%)
MPO	116	-
MPO(CRP)	112	−3.4%
MPO(cTnI)	113	−2.6%
MPO(Myo)	121	4.1%
MPO(CK-MB)	118	1.7%

i_a: Amperometric response to the standard 100 ng mL^{-1} MPO solution. i_b: Amperometric response to the solutions composed of 100 ng mL^{-1} MPO and 1 mmol L^{-1} interfering chemicals respectively.

reaction, which was evaluated as the following equation: $\Delta i_{pa} = i_0 - i_n$, where i_0 is the response current before the immunoreaction and i_n is the response current after the immunoreaction (n = 20, 50, 80, 100 ng mL^{-1}). When the concentration of MPO increased, the amount of immunocomplex also increased. Thus, the observed current signal decreased with increasing concentration of MPO. This resulted in an increase in the change of oxidation peak current response (Δi_{pa}).

As shown in Fig. 5, the current change before and after the immunoreaction was proportional to the concentration of MPO in the linear range of 5 to 300 ng mL^{-1} and the linear regression equation is $\Delta i_{pa}(\mu A) = 1.44933 + 0.04587C$ (ng mL^{-1}) with a detection limit of 0.2 ng mL^{-1} at a signal to noise ratio of 3δ (where δ is the standard deviation of a blank solution, n = 10, r = 0.99466). When the MPO concentration is higher than 300 ng mL^{-1}, an appropriate dilution of the sample is necessary in the preincubation step.

Reproducibility, selectivity and stability. Reproducibility, selectivity and stabiity are important characteristics of an immunosensor. The reproducibility of the immunosensor was evaluated by intra- and inter-assay coefficients of variation (CVs). The intra-assay precision of the analytical method was evaluated by analyzing 3 concentration levels (high, middle and low) 6 times per run. The CVs of intra-assay with this method was 3.3%, 4.1% and 3.8% at 200, 80 and 10 ng mL^{-1} of MPO solution, respectively. Similarly, the inter-assay CV on five immunosensors used independently was 3.8, 5.1 and 4.3% for 200, 80 and 10 ng mL^{-1} of MPO solution, respectively. To examine the specificity of the immunosensors, the immunosensors were immersed into 100 ng mL^{-1} MPO solution in the presence of 1.0 mmol L^{-1} CRP, cTnI, Myo and CK-MB, respectively. The results, shown in Table 1, suggested that these chemicals with concentrations below those of normal human serum samples did not interfere with MPO detection. The stability of the immunosensor was also investigated. When the immunosensor was stored in the refrigerator at 4 °C after 20 days, it retained 90% of its initial response.

Regeneration. In our experiment, immunosensors were regenerated by immersing into 8 mol L^{-1} urea solution after each assay was completed, then washed with water to dissociate the antigen-antibody complex. The immunosensor kept 92% of the original current after regenerated six times and the relative standard deviation (RSD) was 3.1%.

Preliminary application of the immunosensor. To investigate the possibility of the immunosensor used for practical analysis, 20 serum samples were examined by the developed immunosensor and the standard ELISA method. As shown in Fig. 6, the regression equation is as follows: y = 4.72462 + 0.92866x, (r = 0.978) (x-axis, concentration of immunosensor; y-axis, concentration of ELISA), which indicates that the developed immunosensor are feasible to detect MPO in human serum for clinical diagnosis.

Conclusion

In this present work, we fabricate an amperometric immunosensor for the detection of MPO based on the immobilization of anti-MPO on a glassy carbon electrode modified by DMF-MWCNTs-EMIMBF$_4$/chitosan-CeO$_2$ composite membrane, which greatly improves the electrochemical behavior and enhances the sensitivity of the immunosensor. This method has several advantages such as high sensitivity, a wide linear detection range for the detection of MPO and no need for multiple labeling procedure. Importantly, because this approach does not require sophisticated fabrication procedure, it is well suited for point-of-care testing and self-monitoring in both clinical and scientific research areas.

Acknowledgments. This work was supported by the Fund of Science and Technology Development of Chongqing (CSTC-2009AC5145).

References

1. Eiserich, J. P.; Baldus, S.; Brennan, M. L.; Ma, W. X.; Zhang, C. X.; Tousson, A.; Castro, L.; Lusis, A. J.; Aldons, J.; William, M. N.; White, C. R.; Freeman, B. A. *Science* **2002**, *296*, 2391.
2. Wang, Z. N.; Nicholls, S. J.; Rodriguez, E. R.; Kummu, O.; Horkko, S.; Barnard, J.; Reynolds, W. F.; Topol, E. J.; DiDonato, J. A.; Hazen, S. L. *Nat. Med.* **2007**, *13*, 1176.
3. Meuwese, M. C.; Stroes, E. S. G.; Hazen, S. L. *J. Am. Coll Cardiol.* **2007**, *50*, 159.
4. Morrow, D. A.; Sabatine, M. S.; Brennan, M. L.; de Lemos, J. A.; Murphy, S. A.; Ruff, C. T.; Rifai, N.; Cannon, C. P.; Hazen, S. L. *European Heart Journal* **2008**, *29*, 1096.
5. Libby, P. *Nat.* **2002**, *420*, 868.
6. Baldus, S.; Heeschen, C.; Meinertz, T. M.; Zeiher, A. M.; Eiserich,

J. P.; Münzel, T.; Simoons, M. L.; Hamm, C. W. *Circulation* **2003**, *108*, 1440.
7. Brennan, M. L.; Penn, M. S.; Lente, F. V.; Nambi, V.; Shishehbor, M. H.; Aviles, R. J.; M, M. G.; Pepoy, M. L.; McErlean, E. S.; Topol, E. J.; Nissen, S. E.; Hazen, S. L. *N. Engl. J. Med.* **2003**, *349*, 1595.
8. Tang, D.; Yuan, R.; Chai, Y. *Anal. Chem*. **2008**, *80*, 1582.
9. Fu, X. H.; Wang, J. Y.; Li, N.; Wang, L.; Pu, L. *Microchim. Acta* **2009**, *165*, 437.
10. Zhang, T. T.; Yuan, R.; Chai, Y. Q.; Liu, K. G.; Ling, S. J. *Microchim Acta* **2009**, *165*, 53.
11. Pandey, P.; Singh, S. P.; Arya, S. K.; Gupta, V.; Dutta, M.; Singh, S.; Malhotra, B. D. *Langmuir* **2007**, *23*, 3333.
12. Pingarro, J. M,; Sedeno, P. Y. *Electrochim. Acta* **2008**, *53*, 5848.
13. Tang, H.; Chen, J. H.; Yao, S. Z.; Nie, L. H.; Deng, G. H.; Kuang, Y. F. *Anal. Biochem.* **2004**, *331*, 89.
14. Joo, S. H.; Choi, S. J.; Oh, I.; Kwak, J.; Liu, Z.; Terasaki, O.; Ryoo, R. *Nat.* **2001**, *412*, 169.
15. Wei, A.; Sun, X. W.; Wang, J. X.; Lei, Y. C.; X, P.; Li, C. M.; Dong, Z. L.; Huang, W. *Appl. Phys. Lett.* **2006**, *89*, 123902.
16. Wang, J. X.; Sun, X. W.; Wei, A.; Lei, Y.; Cai, X. P.; Li, C. M.; Dong, Z. L. *Appl. Phys. Lett.* **2006**, *88*, 233106.
17. Sun, W.; Li, X. Q.; Liu, S. F.; Jiao, K. *Bull. Korean Chem. Soc.* **2009**, *30*, 582.
18. Wang, L. G.; Xu, J. J.; Chen, H. Y.; Fu, S. Z. *Biosens. Bioelectron.* **2009**, *25*, 791.
19. Ansari, A. A.; Kaushik, A.; Solanki, P. R.; Malhotra, B. D. *Electrochem. Commun*. **2008**, *10*, 1246.
20. Ansari, A. A.; Solanki, P. R.; Malhotra, B. D. *Appl. Phys. Lett.* **2008**, *92*, 263901.
21. Xiao, X. L.; Luan, Q. F.; Yao, X.; Zhou, K. B. *Biosens. Bioelectron.* **2009**, *24*, 2447.
22. Mehta, A.; Patil, S.; Bang, H.; Cho, H. J.; Seal, S. *Sens. Actuators, A* **2007**, *134*, 146.
23. Kaushik, A.; Solanki, P. R.; Ansari, A. A.; Ahmad, S.; Malhotra, B. D. *Nanotechnol.* **2009**, *20*, 055105.
24. Feng, K. J.; Yang, Y. H.; Wang, Z. J.; Jiang, J. H.; Shen, G. L.; Yu, R. Q. *Talanta.* **2006**, *70*, 561.
25. Ansari, A. A.; Solanki, P. R.; Malhotra, B. D. *J. Biotechnol.* **2009**, *142*, 179.
26. Islam, M.; Ferdousi, B.; Okajima, T.; Ohsaka, T. *Eletrochem Commun*. **2005**, *7*, 789.
27. Lu, X.; Zhang, Q.; Zhang, L.; Li, J. *Electrochem Commun.* **2006**, *8*, 874.
28. Zhang, W.; Yang, T.; Zhuang, X. M.; Guo, Z. Y.; Jiao, K. *Biosens. Bioelectron*. **2009**, *24*, 2417.
29. Aziz, A.; Yang, H. *Bull. Korean Chem. Soc.* **2007**, *28*, 1171.
30. Yang, X. F.; Gan, T. Zheng, X. J.; Zhu, D. Z.; Wu, K. B. *Bull. Korean Chem. Soc*. **2008**, *29*, 1386.
31. Kang, X. H.; Wang, J.; Wu, H.; Aksay, I. A.; Liu, J.; Lin, Y. H. *Biosens. Bioelectron*. **2009**, *25*, 901.
32. Lee, C. A.; Tsai, Y. C. *Sens. Actuators B* **2009**, *138*, 518.
33. Fukushima, T.; Kosaka, A.; Ishimura, Y.; Yamamoto, T.; Takigawa, T.; Ishii, N.; Aida, T. *Science* **2003**, *300*, 2072.